Sustainable Cities and Society 62 (2020) 102398

Contents lists available at ScienceDirect

Sustainable Cities and Society

journal homepage: www.elsevier.com/locate/scs

Probabilistic modeling of cascading failure risk in interdependent channel and road networks in urban flooding

Shangjia Dong[a,*], Tianbo Yu[b], Hamed Farahmand[c], Ali Mostafavi[c]

[a] Department of Civil and Environmental Engineering, University of Delaware, Newark, DE 19716, United States
[b] Department of Electrical and Computer Engineering, Texas A&M University, College Station, TX 77843, United States
[c] Zachry Department of Civil and Environmental Engineering, Texas A&M University, College Station, TX 77843, United States

ARTICLE INFO

Keywords:
Co-located channel-road network
Bayesian network modeling
Urban resilience
Cascading failure
Probabilistic flood risk assessment

ABSTRACT

This paper presents a probabilistic model for assessing risk of cascading failures in co-located road and channel networks. The proposed Bayesian network analysis framework integrates network structural properties and empirical flood propagation data to model the spread of flooding. The model was tested in a multiple watershed scenario in Harris County, Texas (USA), using historical flood data from past events. The results show the capability of the proposed Bayesian network model to quantitatively characterize the failure (i.e., inundation) of road network considering the cascading failure (i.e., overflow) from the channel network. The proposed model also enables simulating the risk of flood cascades (i.e., flood propagation) on the road network with high accuracy. The generic design of the algorithm also enables the adaptation of the proposed framework in other cities and regions. Accordingly, the proposed model provides a new tool to help decision-makers prioritize infrastructure protection plans and emergency response actions.

1. Introduction

Road networks serve as the backbone of the modern city to transport people and goods, disruption of which will severely impact the well-being of our urban system, e.g., access to medical care (Dong, Esmalian, Farahmand, & Mostafavi, 2020; Dong, Wang, Mostafavi, & Gao, 2019), road transport (Yang, Ng, Zhou, Xu, & Li, 2019a), social cohesion, and economic development (Taylor, 2012). Road disruptions can result from both internal dynamics (e.g., road closure, traffic accidents, infrastructure aging, and traffic congestion) and external stressors (e.g., floods, landslides, wildfires, heavy snowfall, hurricane, storms, earthquakes, etc.). Disruptions caused by natural disasters presents a larger scale of damage on road networks (Jenelius & Mattsson, 2015). Not only have our urban infrastructure system became more complex but also the intensity and frequency of natural disasters have increased over the past decade. This makes road network extremely susceptible to disruptions that can result in considerable serviceability reduction (Batouli & Mostafavi, 2018; Berdica, 2002; Rasoulkhani & Mostafavi, 2018). Understanding the risk that road networks face in natural disasters can significantly help decision-makers to derive critical infrastructure protection strategies to support rescue strategy prioritization and emergency management (Jenelius, Petersen, & Mattsson, 2006).

Among the catastrophic natural disasters, flooding, in particular, cause extensive economic losses and posed a great threat to the well-being of communities. For example, Hurricane Harvey made landfall in Harris County, Texas in 2017 and resulted in $125 billion losses and 4.37 million people were affected (HCFCD, 2019). With the growing urbanization and climate change, global exposure to floods is expected to increase threefold (Aerts et al., 2018). Floods cause significant disruptions in road networks. The co-location dependencies between channels and road networks make road networks particularly vulnerable to cascading failures in flood channels. Channels refer to the rivers, creeks, and bayous that discharge the rainfall runoff. Here, co-location dependency is defined as the closeness in distance between channel and road intersections (Goldbeck, Angeloudis, & Ochieng, 2019; González, Sánchez-Silva, Due nas-Osorio, & Medaglia, 2014; Thacker, Barr, Pant, Hall, & Alderson, 2017). Cascading failure refers to the failure of flood control network when water level exceeds the bank of the channel and then leads to the water flowing and spreading on the road network. While the co-location dependencies between channel and road networks have been recognized in the existing literature (Klinkhamer et al., 2017), there is a lack of models to analyze failure cascade risk in co-located road and channel networks. In order to address this gap, this

* Corresponding author.
E-mail addresses: sjdong@udel.edu (S. Dong), tianbo@tamu.edu (T. Yu), hamedfarahmand@tamu.edu (H. Farahmand), amostafavi@civil.tamu.edu (A. Mostafavi).

https://doi.org/10.1016/j.scs.2020.102398
Received 11 January 2020; Received in revised form 10 July 2020; Accepted 11 July 2020
Available online 14 July 2020

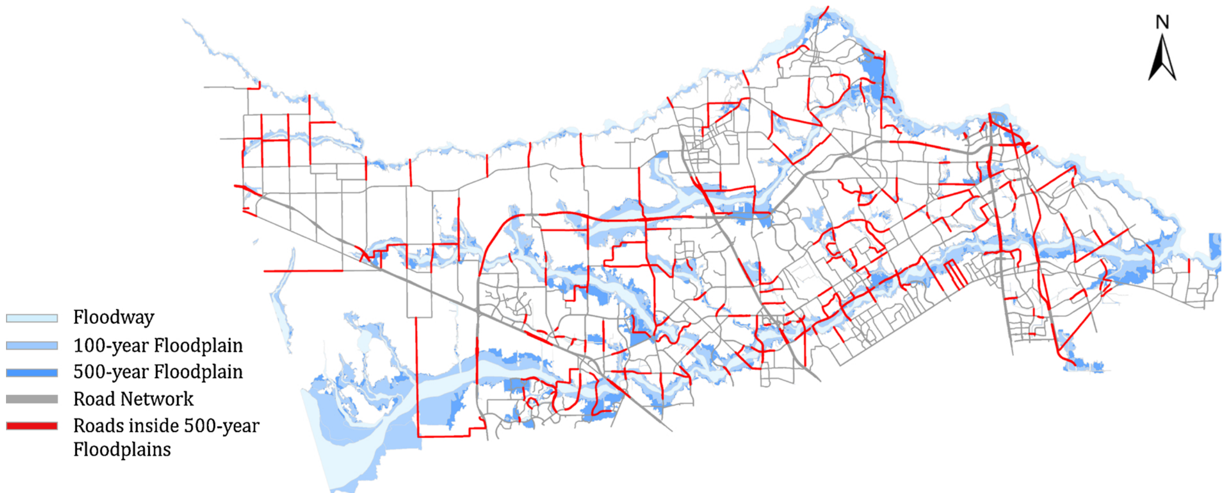

Fig. 1. Floodplain-identified vulnerable roads in risk of flooding.

paper proposed a new Bayesian Network analysis methodology to analyze cascading failure risks in road networks facing urban flooding. The application of the proposed method is demonstrated in Harris County (Texas, USA) as a test-bed.

1.1. Current approaches to roads flood risk assessment

The standard approach for assessing road network flood risk is using hydraulic and hydrologic (H&H) models (Al-Sabhan, Mulligan, & Blackburn, 2003; Itoh, Ikeda, Nagayama, & Mizuyama, 2018). Overlaying the generated flood map on road networks, vulnerable roads can be identified. Fig. 1 shows the identified vulnerable roads obtained by overlaying Federal Emergency Management Agency (FEMA) 100-year and 500-year floodplain maps. There are in total of 733 roads are in the vicinity of floodplains and can be deemed as vulnerable roads as they are exposed to high risk of flooding. This static approach is commonly used in making land-use plans and assessing the plan integration (Berke, Malecha, Yu, Lee, & Masterson, 2019) as it directly identifies vulnerable infrastructures. However, flood plains do not fully capture risk exposure of road networks since flood risk can extend beyond the standard boundaries of flood zones (plains) (Aerts et al., 2018). During Hurricane Harvey, for example, almost three-quarters of the homes damaged in Harris County were situated outside the federally regulated 100-year floodplain. During Tax Day floods in 2016 (in Harris County), more than 55 percent of the homes damaged were located outside of the 500-year floodplain. In the Memorial Day floods in 2015 (in Harris County), more than one-third of the homes damaged were outside of the 500-year floodplain (HCFCD, 2019). These flooding events caused road inundations and disrupted access in areas outside flood plains. Hence, despite the practical value and convenient employment of floodplain maps, overlaying floodplains on road networks provides limited insight into failure cascade risk to inform emergency response prioritization and infrastructure failure early warning.

1.2. Co-location dependencies between channel and road networks

Infrastructure systems are becoming increasingly interdependent, small failure in one system can propagate to its dependent counterpart and results in cascading failure (Dong, Wang, Mostafizi, & Song, 2020; Saidi, Kattan, Jayasinghe, Hettiaratchi, & Taron, 2018; Zhu et al., 2017). In an urban system, different infrastructures are built surrounding the roads to take advantage of service transport (e.g., warehouse), access to resources (e.g., gas, water, food, etc.) and also to protect infrastructure from damage (Rahimi, Dehghani, & Shafieezadeh, 2019). In flood-prone areas, road and channel networks are highly interdependent due to their co-location (Saidi et al., 2018). Channel networks protect urban areas (and roads) from flooding by draining stormwater, and roads become part of channel networks when flood water spreads in urban areas. Such co-location dependency has exposed road networks to high risk of cascading failure (road inundations caused by water overflow from channel networks). Such increased flood risk due to co-location of channel and road networks is, however, rarely examined in the road network vulnerability assessments. In particular, depending on the geographic location and topological property of flood control network, the likelihood of flooding in different regions varies (Dong, Wang, et al., 2020). For example, certain flood control infrastructure shows larger probability of failure during flooding due to its topological location in the network. The co-location dependency would further affect the likelihood of flooding in roads located in the proximity of channel networks. However, the existing road network vulnerability assessment methods do not capture this co-location dependency and the resulting spatial-temporal cascading failure risks. To address this gap, this study presents a probabilistic approach to capture the failure cascade dynamics in co-located channel-road networks.

1.3. Point of departure

Road network analysis models examine the roadway infrastructure as a network of nodes (i.e., intersections) and links (i.e., roads) (Dong, Mostafizi, Wang, Gao, & Li, 2020; Jenelius & Mattsson, 2015). Road network vulnerability has been studied from many different perspectives. For example, using topological measures of the network, Jenelius et al. (2006) introduced link importance and site exposure to measure the vulnerability of road network of northern Sweden. Considering the socio-economic impacts of network, Taylor (2012), Taylor, Sekhar, and D'Este (2006) incorporated accessibility and remoteness in examining the vulnerability of the regional road network. Concerning the transport-related and direct financial consequences of road failures, Erath, Birdsall, Axhausen, and Hajdin (2009) examined the vulnerability of Swiss road network. Furthermore, as the complex infrastructure interaction is becoming increasingly important in the healthy functioning of urban systems, recent studies are also including the interdependency component in the vulnerability assessment of technical infrastructures. Dong, Wang et al. (2020) modeled the interdependency between sewer and road network and examined the road network vulnerability/robustness in facing large-scale earthquake disruptions. Johansson and Hassel (2010) employed both graph theory-inspired geographical and functional interdependency to model a fictional electrified railway network that comprises five interdependent systems and assess the vulnerability of the interdependent systems. However, these road vulnerability assessment methods are mainly the topology-based models and use fictional disruption scenarios. In addition, road network vulnerability assessments in face of the natural hazards (e.g., urban flood) normally use simulated scenarios such as 1-in-year rainfall event. Despite the valuable vulnerable asset identification, they do not explicitly consider the co-location interdependency between road and channel network and incapable of incorporating empirical data to validate the proposed model (Singh, Sinha, Vijhani, & Pahuja, 2018). This research is primarily motivated by the fact that standard network-based road flood risk analysis considers neither the historical flood data in different regions nor the influence of the structure of co-located channel and road networks, while H&H models provide limited insights about the spatial-temporal failure cascade of the interdependent networks. Hence, the existing methods have major limitations to inform response strategy prioritization, emergency management, and hazard mitigation decisions.

To address this important gap, this study proposes a probabilistic graphical model, Bayesian network model, to capture the interaction between channel and road networks and their co-location dependency. To test the proposed method, data from three empirical flood events in Harris County (2016 Tax Day Flood, 2016 Memorial Day Flood, and 2017 Hurricane Harvey Flood) were utilized to train and test the model. The trained Bayesian network is capable of characterizing the spatial-temporal failure cascade (i.e., flood propagation) in the road network with high accuracy. In addition, compared to the standard binary approach for vulnerable roads identification, the derived cascading failure risk of road network in urban flooding employs a system perspective by considering co-location interdependencies (Little et al., 2019; Mostafavi, 2017, 2018) and provides a quantitative measure, which informs emergency response decisions. The proposed Bayesian network model complements H&H models and topological-based vulnerability analysis by providing more data-driven and real-time prediction capabilities. In particular, the proposed Bayesian network-based modeling of interdependent channel-road networks is able to dynamically capture the inundation propagation and provide predictive early flood warning to communities in near real-time.

The remainder of the paper is organized as follows. Section 2 reviews the related literature on road network risk and vulnerability assessment and the application of Bayesian network modeling. Section 3 presents the framework of the proposed methodology and the detailed execution procedure. Section 4 shows the application of proposed framework through a case study in Harris County. Finally, Section 5 concludes the paper with significant findings and future research directions to improve the analysis.

2. Review of road network vulnerability assessment methods

Road network vulnerability has been extensively examined in the existing research. This section provides a review of the existing methods and their limitations. First, Studies focusing on investigating road network vulnerability in other contexts (e.g., travel reliability, mobility, accessibility, etc.) are discussed. Then, we discuss the studies that have used Bayesian network modeling for network vulnerability analysis in other infrastructure and hazards. Based on these discussions, we demonstrate the need for the proposed Bayesian network modeling of co-located channel-road network for cascading failure risk characterization in urban flooding.

2.1. Road network risk and vulnerability assessment

Risk is often considered as a product of the vulnerability of the system, severity or frequency of the hazards, and exposure to hazards (Birkmann, 2007; Joyce, Chang, Harji, & Ruppert, 2018). Accordingly, flood risk assessment in road networks should consider the vulnerability of infrastructure networks, severity or frequency of flood scenarios, as well as the exposure of the infrastructure segments to inundation (Lyu, Shen, Zhou, & Zhou, 2019). Although in the context of risk assessment, vulnerability is often evaluated based on economic consequences and losses of the hazard, there are other indicators that can properly capture the vulnerability of road networks from a system-level perspective (Yin, Yu, Yin, Liu, & He, 2016). System-level road network vulnerability assessment has been a major focus in both transportation engineering and disaster science research (Mostafavi & Ganapati, 2019). The definition of vulnerability, however, varies in different contexts. For example, Taylor et al. (2006) argue that the network weakness and consequences of failure determine the network vulnerability. Nevertheless, road network vulnerability is often attributed to the reduced accessibility (Berdica, 2002), which is measured by connectivity loss, travel delay, and network flow capacity drop (Chang, Peng, Ouyang, Elnashai, & Spencer, 2012; Dong, Wang et al., 2019; Sullivan, Novak, Aultman-Hall, & Scott, 2010). Many studies have been focusing on analyzing the network vulnerability through network topological properties (Dey, Gel, & Poor, 2019; Dong, Esmalian et al., 2020; Dong, Wang et al., 2020). A network's response to a disruption in the form of activity-travel behavior changes or (and) simulating the impacts of disruptions (Dong, Wang et al., 2020; Erath et al., 2009; Konduri et al., 2013) are used to represent the network vulnerability. In both cases, a proper network disruption (e.g., disaster-induced failure propagation) model is required.

There are various hazard models developed to simulate the failure propagation and measure network vulnerability. These models consider the severity and frequency of the hazard and characterize the spatio-temporal propagation of failures. For example, Mostafizi, Wang, Cox, Cramer, and Dong (2017) modeled road network disruption using an agent-based tsunami inundation model that determines time-dependent water depth and flow speed in the hazard zones. Wang, Yang, Stanley, and Gao (2019) introduced a flood-induced road network failure percolation framework using a flood simulator that employs a global river model to generate floods with different intensities to study the robustness phase transition in road networks. Dong, Esmalian et al. (2020) modeled the network failure by removing nodes and links (i.e., intersections and roads) that are potentially impacted by the flooding in which the distance to the flood control network is converted to represent the hazards exposure of road infrastructure. Yang et al. (2019b) used existing intensity-duration-frequency (IDF) rainfall curves to model inundation propagation in an interdependent stormwater drainage-road network model.

In the context of urban flooding, the standard approach for failure propagation and risk assessment is using H&H models (Al-Sabhan et al., 2003; Itoh et al., 2018). In these models, flow rates are often estimated using rainfall-runoff and streamflow projecting models (Gori, Blessing, Juan, Brody, & Bedient, 2019; Lü et al., 2013). Using H&H models, the risk of road segments to flood inundation is often measured by overlying flood inundation maps on the road networks. This approach, however, has several limitations. First, creating a site-specific H&H model requires collecting data such as the topography of the study area, soil characteristics, land use, hydrologic variables, which can be prohibitive due to the extensive data collection effort. Second, running these models can be computationally demanding and time-consuming since they require multiple tests to provide a comprehensive vulnerability assessment. Third, despite the accurate flood depth and area estimation, H&H models do not provide spatial-temporal dynamics of the flood cascading. All these limit the use of these models as a real-time decision-support tool for emergency response.

In the case of urban fluvial flooding, the main contributor to road network failure (i.e., inundation) is the propagation of the overflow from channels and rivers to road. This cascading failure is further exacerbated when urbanization increased transportation infrastructure development in the vicinity of the flood control network. Different studies have employed H&H models to investigate urban flooding. For example, Seyoum, Vojinovic, Price, and Weesakul (2012) presented a two-dimensional model that coupled with a one-dimensional sewer network model (SWMM5) and it was tested on one hypothetical case study and one real-life case study of Bangkok. Chang, Wang, and Chen (2015) integrated the one-dimensional sewer flow model and two-dimensional overland flow model considering different types of land cover of the study areas. Both of these studies present promising results in predicting the inundation depth and area. The insights obtained from H&H models could be complemented using data-driven models. In particular, data-driven models could provide better insights regarding failure cascade risks in road networks as a flood event unfolds. In addition, with the advancement of sensor technology and computing power and constant change in the built-environment, empirical data encapsulates the most up-to-date information regarding a region. The proposed Bayesian network-based modeling of interdependent channel-road networks is able to dynamically capture the inundation propagation and provide the early flood warning to communities in danger in near real-time. To the best of the authors' knowledge, there is no existing network-based model in the literature that considers the road-channel co-location interdependence to characterize vulnerability and spatial-temporal failure cascade risk in road networks.

2.2. Bayesian network modeling for vulnerability assessment

Amongst the most popular methods for probabilistic modeling of interdependent networks (Rahnamay-Naeini & Hayat, 2016), Bayesian network model is one of the powerful probabilistic graphical models that enable the integration of both dependencies and uncertainties in network vulnerability assessment (Di Giorgio & Liberati, 2012). Bayesian network models consist of nodes and edges, where nodes generally represent variables and edges show the conditional dependence between variables (Špačková & Straub, 2013; Scutari & Nagarajan, 2013). In a Bayesian network model, the state of a subset of variables can be updated when the status of other observed variables (evidence) are known using Bayes' theorem (Grande, Castillo, Mora, & Lo, 2017; Saliminejad & Gharaibeh, 2012). In Bayesian network modeling, the posterior distribution of investigating variables given evidence is calculated in the process of probabilistic inference, which can be solved by different algorithms such as variational message passing, and unscented message passing (Winn & Bishop, 2005).

Bayesian network models have been used for infrastructure vulnerability assessment (Hosseini & Barker, 2016; Khakzad, 2015; Oh, Deshmukh, & Hastak, 2010). For example, Bayesian network modeling has been used to detect common damage configurations in a road network (Gehl, Cavalieri, Franchin, & Negulescu, 2017) and multi-hazard vulnerability assessment in bridge systems (Gehl & D'Ayala, 2016). Applegate and Tien (2018) employed Bayesian network modeling to conduct probabilistic vulnerability analysis in coupled power-water networks. Bayesian network has also been used for flood risk assessment (Joo et al., 2019). For example, Li, Wang, Leung, and Jiang (2010) developed a Bayesian network-based risk assessment framework for flood control infrastructure. Abebe, Kabir, and Tesfamariam (2018) constructed a Bayesian belief network model by identifying different factors that impact the risk of pluvial flood in urban areas and developed a spatial measure to help compare flood risk in different areas. Chen, Zhong, An, Zhu, and Xu (2019) also adopted Bayesian network model to analyze the risk in real-time operation of reservoir systems contributing to flooding protection. Dong, Yu, Farahmand, and Mostafavi (2019) used the Bayesian network model to characterize the failure cascade and assess the vulnerability flood control network. Narayan, Simmonds, Nicholls, and Clarke (2018) used the Bayesian network model to assess the risk of inundation in different paths in coastal areas under different probabilities. While these studies have shown the capability of Bayesian network modeling in the context of flood risk assessment, their focus has not been on examining vulnerability and failure cascade risk in co-located channel and road networks.

In the case of road network vulnerability assessment facing urban fluvial flooding, Bayesian network modeling offer two important capabilities. First, Bayesian network enable capturing associated uncertainties (Tasdighi, Arabi, Harmel, & Line, 2018) and infrastructure risk in different sub-models to consider the impact of hazards on infrastructures (Bensi, Der Kiureghian, & Straub, 2011), which provides a great risk-informed decision-making tool (Chen et al., 2019). Second, various forms of infrastructure dependencies and interdependencies can be properly integrated using Bayesian network (Haraguchi & Kim, 2016). Especially, Bayesian models enable modeling propagation of failure within an infrastructure system as well as propagation of failure across interdependent infrastructure systems (Hossain, Jaradat, Hosseini, Marufuzzaman, & Buchanan, 2019). Recognizing these capabilities, this study proposes a Bayesian network model that incorporates the topology of the co-located flood control and road network, along with the associated causal and influential relationships. In the proposed framework, the effects of the network topology, hydrological parameters, such as rainfall and stream elevation, and their relationship with inundation status can be captured using probabilistic inference. This modeling framework enables a system-level vulnerability assessment and accurate characterization of failure cascade in the road networks in the face of urban fluvial flooding.

3. Methodology

The proposed model incorporates the topology of channel and road networks, along with their co-location dependency, to map and build the Bayesian network structure. The Bayesian network model also takes advantage of historical sensor data to characterize failure cascades (i.e., inundation) on a road network facing urban fluvial flooding. The proposed model is elaborated through the use of a case study in Harris County, Texas (USA). Fig. 2 shows the overview of Bayesian network

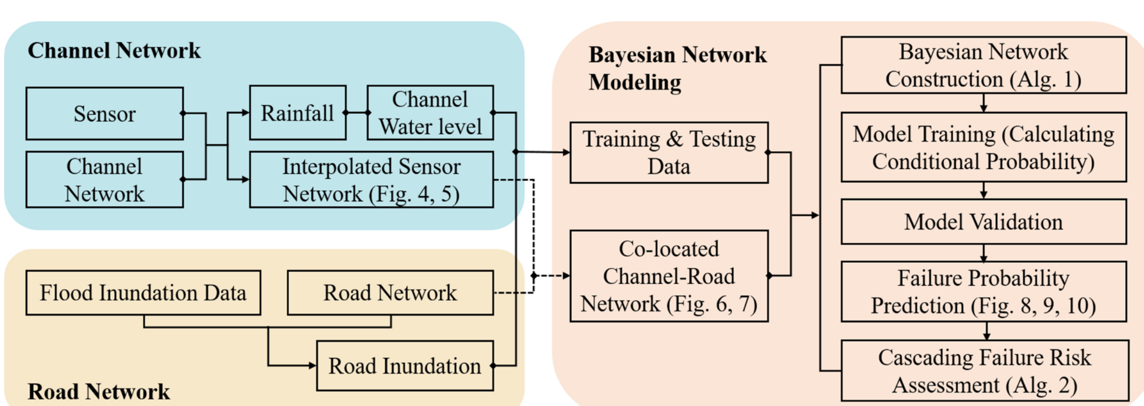

Fig. 2. Framework of Bayesian network modeling of co-located channel-road network.

modeling framework for co-located channel-road network cascading failure risk characterization during urban flooding. Empowered by modern sensor technology, Harris County deployed over 150 sensors across the network to monitor the flooding status of major channels. This study used the sensor data to train and validate the model using historical flood sensor data. The proposed framework mainly consists of three steps: (1) mapping and enriching the channel network and interpolating the flooding status of the intermediate channel components based on the existing sensors; (2) constructing the co-location dependency relationship between the channel network and road network; and (3) predicting road failure (inundation) probability based on the sensor-collected inundation information from the channel network to assess the road network cascading failure probability.

3.1. Channel network mapping

Knowing flood information for all the channels is ideal for better assessment of failure cascade (i.e., overflow) in the channel network. Due to the high maintenance and cost of the sensors, it is likely that not all channels are monitored with flood gauge sensors. Harris County Flood Control District (HCFCD), for instance, only deployed 175 sensors across the network to monitor the flooding status of major channels. The number of sensors in the network is far from adequate. In the northwest region of Harris County (shown in Fig. 3), a combined watershed (i.e., Cypress Creek, Little Cypress Creek, Willow Creek, and Spring Creek) comprises 583 km of channels with only 28 sensors installed. Due to the limited number of sensors and large spans between two sensors, only using the channel components with flood sensors would lead to losing the topology integrity of the channel network and it would further lead to a very sparse dependent channel-road network structure which makes it hard to accurately predict the flooding status of the road intersections between two flood sensors. Therefore, to enrich the resolution of flood status information in the channel network based on existing sensors, we selected qualified intermediate channel components between two existing sensors as a hypothetical sensor to monitor the flooding status during different flood events. Fig. 5 shows an illustrative example of the intermediate channel component construction process.

Due to the limited sensors on the channel network, not every flood

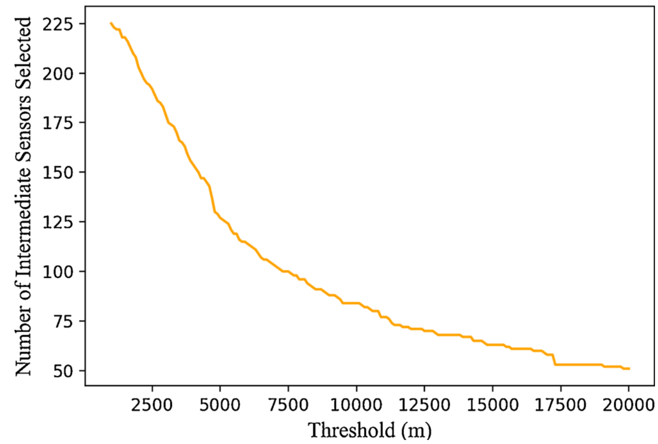

Fig. 4. Relationship between distance threshold setting and selected number of intermediate sensors.

control infrastructure is monitored. The core channel network is first constructed by mapping sensors to its nearest channel component (shown in Fig. 5(a)). Essentially, the core channel network is a network of sensors that are connected by the channels. Next, a qualified channel component is selected when the distance between the component of interest and all the sensors and already-selected components is larger than a certain defined threshold. A small distance threshold can result in excessive component density, which could lead to a significant increase in both the time and space complexity of the Bayesian network model. On the other hand, a large distance threshold would lead to a sparse core flood control network, which can affect the accuracy of failure cascade characterization. Fig. 4 shows the relationship between distance threshold and the number of selected intermediate sensors.

As the distance threshold increases, the number of the intermediate sensors selected decreases. On one hand, with shorter distance, there will be a larger number of intermediate sensors selected, which will further increase the link number in the interdependent networks. As Bayesian network suffers from scaling problem, extensive number of

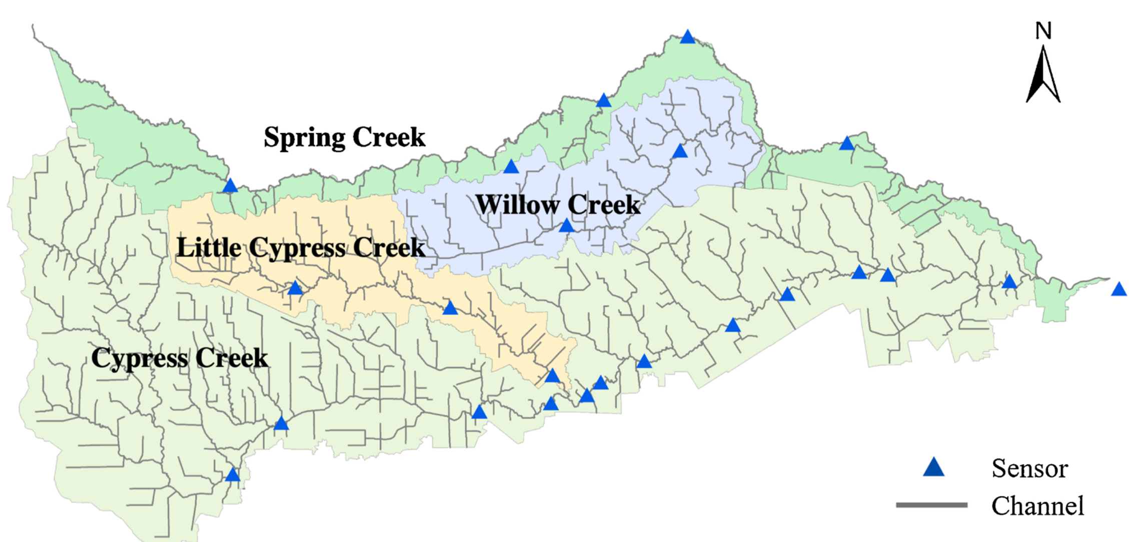

Fig. 3. Sensor distribution in combined watersheds (Cypress Creek, Little Cypress Creek, Willow Creek, and Spring Creek).

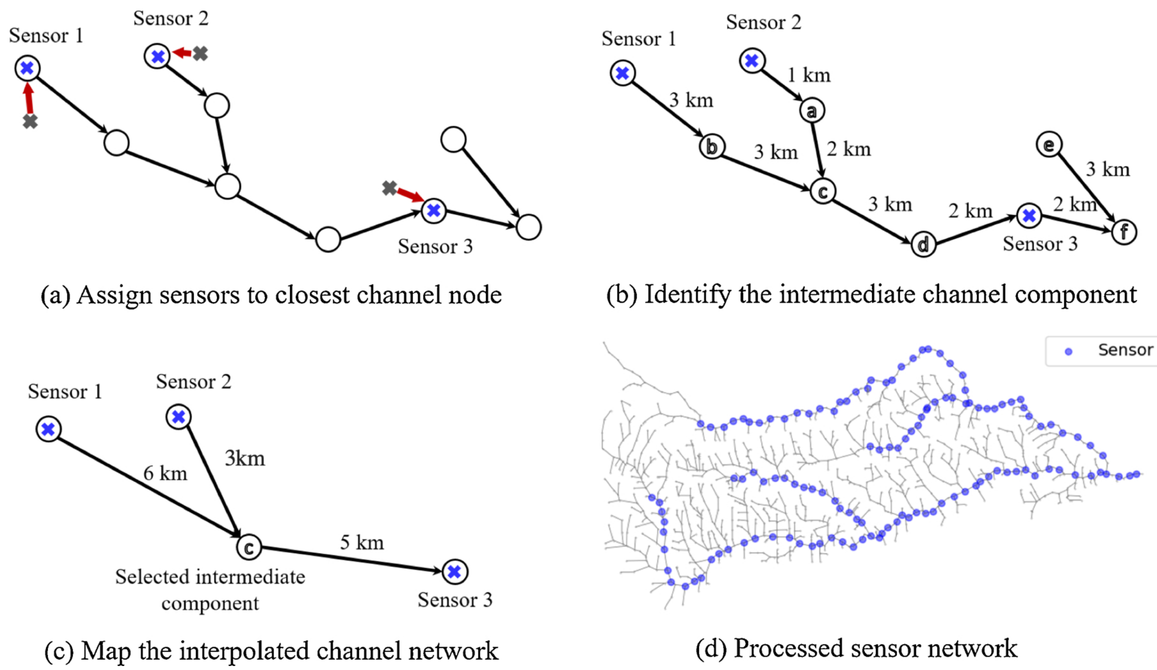

Fig. 5. Intermediate channel component construction process illustration.

network links are not efficient in terms of model computation. On the other hand, high distance thresholds would lead to fewer number of sensors selected than we need to well represent the channel network and provide a good estimation on the channel flow. Therefore, a threshold of 5 km is selected and corresponding 127 sensors are selected to construct the core of the channel network since it achieves a balance between modeling complexity and accuracy in the experiments.

To select the intermediate channel component, we first start at each sensor and move to its downstream components. When the sum of the distance between a channel component and the starting sensor is equal or larger than the threshold (i.e., 5 km), this component is selected and the sum is reset to zero. This iterative process continues until a sensor or a selected component is met in the downstream. Since an intermediate channel component is selected only if there are sensors on both ends, if the sensor is already the last one in the downstream, we restart the searching from another sensor. These selected intermediate channel components are treated equivalent to the existing sensors. Using Fig. 5(b) and (c) as an example. We first start with sensor 1 and component *c* is the only one that satisfies the threshold criteria. Then, we start from sensor 2 and the selection process is terminated by the selected component *c*. When we start from sensor 3, no component is selected due to the absence of sensors or selected components in the downstream. Finally, the only channel component *c* is selected as an intermediate component. Fig. 5(d) shows the obtained final core channel network for constructing the co-located channel-road network. With the intermediate channel component selected in the network, their status are also interpolated using their adjacent sensors based on the assumption that both the rainfall and water level have a linear relationship with distance. The equation for calculating the channel water level is presented in Eq. (1). We tested the interpolation equation by estimating the sensor's water and rainfall level for a point using its upstream and downstream sensors along the same stream and the empirical and estimated results are very similar. Although the linear assumption is not an ideal estimation, we show that it provides a reasonable estimation of water level and rainfall in this case and it could be further improved in the future with more hydrological parameters obtained and incorporated in analyses (Fig. 6).

$$\text{water level} = \begin{cases} \text{water level} + \text{top of channel} - \text{bank} & \text{nearest channel} \\ h_1 + (h_2 - h_1) \times \dfrac{d_1}{d_1 + d_2} & \text{Intermediate channel} \end{cases} \tag{1}$$

3.2. Channel-road co-location dependency construction

Flood control infrastructure is closely built around the road network to protect transportation infrastructure and developed urban areas from inundation. This development philosophy and pattern creates a co-location dependency between channel and road networks. Using the combined watersheds in the northwest of Harris County as an example, 8.3% of the roads have a channel within a distance of 30 feet (30.48 m). With the sensor-interpolated channel network, we can construct the co-located channel-road network. The co-location dependency link from channels to roads is based on the rule of vicinity: the roads and intersections are affected by their nearest channel (shown in Fig. 7). Following Algorithm (1), the analysis iteratively creates the dependency relationship between road intersections and the sensor-interpolated channel network until all the road intersections are included in the co-location model (as in Fig. 8).

Algorithm 1. Co-located channel-road network construction

```
Input: Co-located network G with set of n sensors and their nearest intersections;
Output: Fully mapped co-located network G with sensors and road intersections embedded;
Initialization: h = minimum heap;
for node in G.road_intersection do
    for neighbor in node.neighbors do
        if neighbor.elevation < node.elevation then
            h.push([distance(node, neighbor), node, neighbor]);
        end
    end
end
while !h.empty() AND choose_node.size() < number of intersections do
    [distance, from_node, to_node] = h.front();
    for neighbor in to_node.neighbor do
        if (neighbor.elevation ≤ to_node.elevation) AND (neighbor not in G) then
            h.push([distance(neighbor, to_node), to_node, neighbor]);
            G.add_edge(neighbor,to_node);
        end
    end
end
Return: G
```

3.3. Road failure probability prediction and cascading failure risk assessment

The proposed Bayesian network model of co-located channel-road network enables predicting the failure cascades (i.e., flood propagation

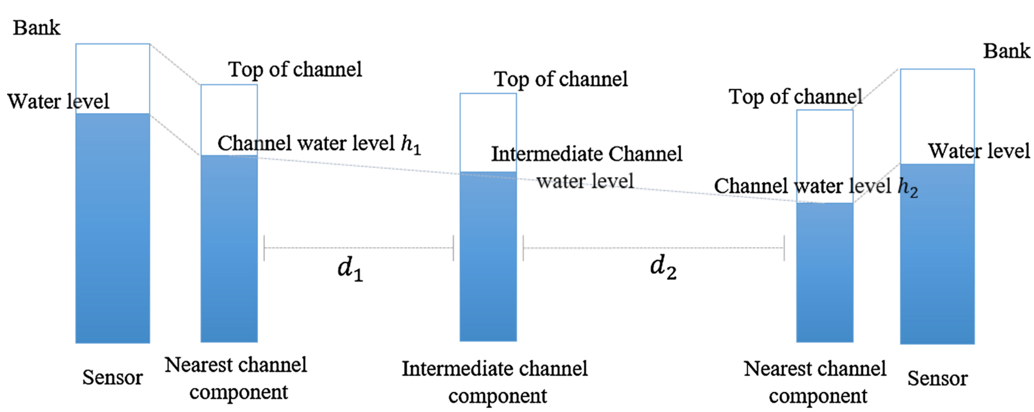

Fig. 6. Intermediate channel component flood information interpolation.

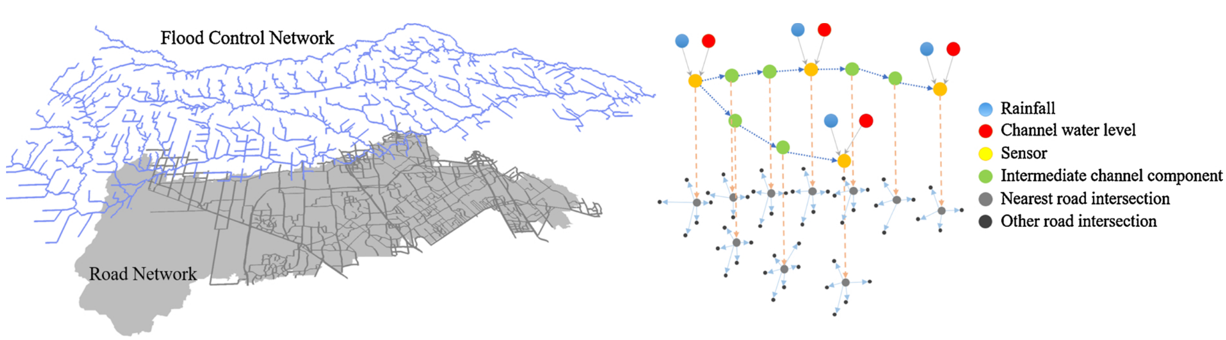

(a) Co-located Flood Control-Road Network

(b) Co-location Dependency Construction

Fig. 7. Co-located channel-road network dependency construction.

Fig. 8. Co-located channel-road network.

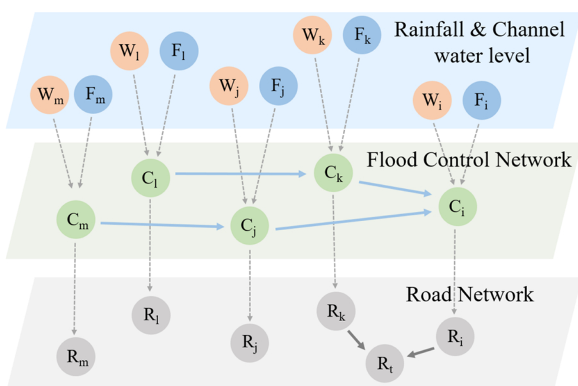

Fig. 9. Bayesian network model structure of co-located channel-road network.

and inundation) in the road network based on the topological relationship and observed evidence (i.e., rainfall, channel water level, and inundation status of nearby sensors and roads). Fig. 9 shows an illustration of the Bayesian network construction of the co-located channel-road networks. R_i is a road intersection of the road network, C_i represents the flooding status of the corresponding channel component, and F_i, W_i are the rainfall and channel water level information observed by C_i, respectively. Essentially, the goal of the model is to calculate the failure probability (i.e., inundation probability) of road intersection, such as R_i and R_t, given flood evidence in a nearby channel and nodal influence.

According to Markov assumption, each node is conditionally independent of its non-descendants if its parents are known. Using the case of Fig. 9 For example, given evidence C_j, F_j and W_j are independent of R_i and they are not considered in the computation of posterior probabilities of R_i. Accordingly, only those variables that are dependent on R_i are involved in the computation of posterior probability and are marginalized out of the conditional probability if they are unknown. Similarly, based on the Markov assumption, if R_i and R_k are known, all other nodes are independent of R_t. Eq. (2) is used to calculates the failure probability of sensor-matched road intersection R_i,

$$
\begin{aligned}
P(R_i|\bar{E} &= \bar{e}) = P(R_i|C_j = c_j, F_i = f_i, W_i = w_i, F_k = f_k, W_k = w_k) \\
&= \sum_{c_k} [P(R_i|C_j = c_j, C_k = c_k, F_i = f_i, W_i = w_i)*P(C_k = c_k|F_k \\
&\qquad = f_k, W_k = w_k)]
\end{aligned} \tag{2}
$$

where the dependent evidence set $\bar{E} = \{C_j, F_i, W_i, F_k, W_k\}$ has observed value $\bar{e} = \{c_j, f_i, w_i, f_k, w_k\}$. Eq. (3) is used for calculating the failure probability of non-directly matched road intersection R_t,

$$
\begin{aligned}
P(R_t|\bar{E}) &= \sum_{r_i, r_k} [P(R_t|R_i, R_k)*P(R_i|R_k, \bar{E})] \\
&= \sum_{r_i, r_k} [P(R_t|R_i, R_k)*[\sum_{c_i, c_k} P(R_i, R_k|C_i, C_k)*P(C_i, C_k|\bar{E})]] \\
&= \sum_{r_i, r_k} [P(R_t|R_i, R_k)*[\sum_{c_i, c_k} P(R_i, R_k|C_i, C_k)*P(C_i|C_k, \bar{E}) \\
&\quad *P(C_k|\bar{E})]] \\
&= \sum_{r_i, r_k} [P(R_t|R_i, R_k)*[\sum_{c_i, c_k} P(R_i, R_k|C_i, C_k) \\
&\qquad *P(C_i|C_j = c_j, F_i = f_i, W_i = w_i, C_k) \\
&\quad * P(C_k|C_l = c_l, F_k = f_k, W_k = w_k)]]
\end{aligned} \tag{3}
$$

The above conditional probability can be computed by Bayes' rule and the failure probability of roads R_t can then be inferred. At each time step, the Bayesian network model calculates the failure probability values for the nodes that have not failed already. Repeating this procedure for each road intersection based on the collected evidence of rainfall, the road failure cascade process can be obtained. The parameters of the Bayesian network model are calculated using maximum likelihood estimation (MLE), which is the default method of the python library pgmpy. MLE estimates the parameters by maximizing the likelihood function. In this case, the condition probabilities are the parameters to be estimated. For example, given a sensor S connected to a road intersection R ($S \to R$), in order to estimate the parameter $\theta = P(R\,|\,S)$, we have thêta = $\text{argmax}_\theta \widehat{L_n}(\theta, y)$, where y is the observed data sample to train the model $y = (S_1, R_1), (S_2, R_2), \ldots, (S_n, R_n)$. With the trained Bayesian network model, we can also evaluate the cascading failure risk of the road network. The risk of each road intersection is calculated based on the flooding probability difference between when its matched sensor is inundated and when its matched sensor is not inundated. This calculation enables us to capture the risk of cascading failure from flood control network to road network. Once the cascading

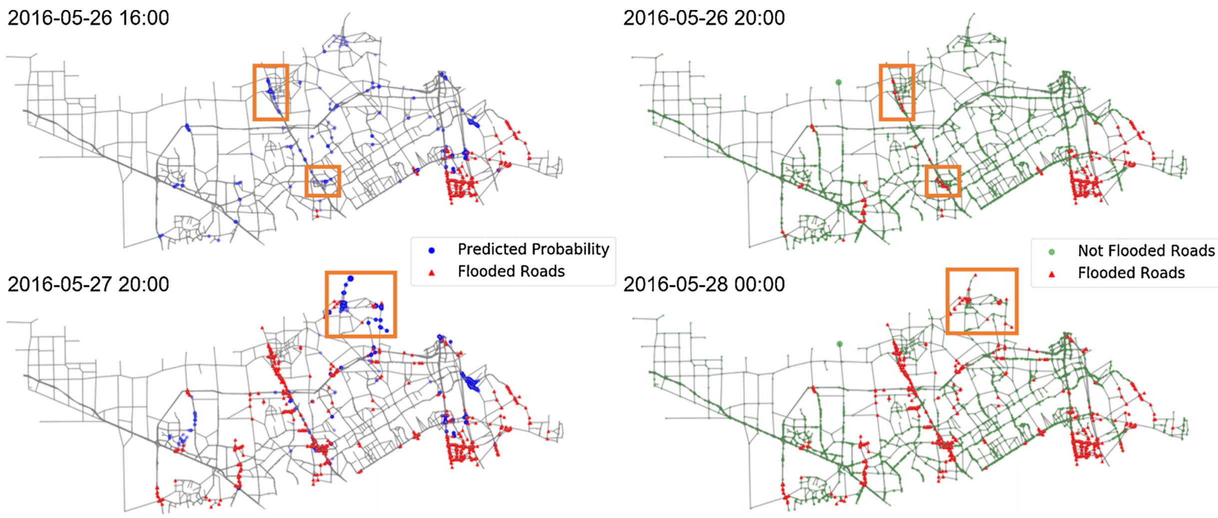

(a) Failure cascade probability forecast (b) Empirical road network failure status

Fig. 10. Temporal road failure cascade illustration. (For interpretation of the references to color in the text, the reader is referred to the web version of this article.)

failure risk of flooding for an intersection is obtained, the risk of a road is calculated by averaging the risk value of intersections at both ends of the road. The cascading failure risk derivation procedure is presented in Algorithm (2).

Algorithm 2. Road network cascading failure risk calculation

Input: Trained Bayesian network model BN with n sensors $s_i, (i = 1, 2, ..., n)$;
Output: Vulnerability index for each road intersections;
Initialization: evidence $e_0 = (s_1 = 0, s_2 = 0, ..., s_n = 0)$;
for *intersection in BN* **do**
  intersection.prob$_{\text{empty}}$ = the probability of intersection to be inundated with e_0;
end
while $i \leq n$ **do**
  $e_i = (s_1 = 0, ..., s_{i-1} = 0, s_i = 0, s_{i+1} = 0, ..., s_n = 0)$;
  for *intersection in* s_i*.connection* **do**
    intersection.prob$_{\text{evidence}}$ = the probability of intersection to be inundated with e_i;
    intersection.vulnerability = intersection.prob$_{\text{evidence}}$ - intersection.prob$_{\text{empty}}$;
  end
  i = i + 1;
end
Return: BN

4. Road network cascading failure risk assessment in Harris County

Harris County, home to Houston, is the third most populous county in the United States and also one of the most flood-prone areas in the country. It has more than 4023 km of channel networks and encompasses 22 watersheds that drain the rainfall-runoff and stormwater to a channel and eventually drains into Galveston Bay. Some watersheds are, however, exposed to higher flood risks and suffered an extensive loss during past flood events. For example, of the 154,170 home flooded during Hurricane Harvey, 8750 houses were from Cypress creek watershed and 4540 houses were from Little Cypress Creek watershed (HCFCD, 2019). Considering its flood risk exposure, we used a combined watershed (as shown in Fig. 3, including Cypress Creek, Little Cypress Creek, Willow Creek, and Spring Creek) in the Northwest region of Harris County as our test-bed for the proposed co-located channel-road Bayesian network model. In total, there are 6353 links and 4061 intersections in the studied road network.

The sensors on the Harris County's flood control network are gradually installed over time. Although the flood record in the Harris County flood warning system can date back to 1989, not enough sensors installed at that time. Therefore, there is a tradeoff between training dataset size and number of the flood sensors. As the distribution of the flood sensors is sparse already, to provide a more accurate flood prediction, we selected 2016 Tax Day Flood (4/16/2016–4/17/2016, 31–41 cm in 12 h), 2016 Memorial Day Flood (5/27/2016–5/28/2016, 20–33 cm in 1 day), and 2017 Hurricane Harvey Flood (8/25/2017–8/31/2017, 71–112 cm in 4 days) as the study flood events to train the Bayesian network model. In addition, of the 28 sensors in the studied watersheds, only data from 20 sensors were utilized in this paper, as some sensors were newly installed after these three flooding events. If all sensors' data are used, some sensors will be fill with empty flooding record, which can severely affect the model's flood prediction accuracy.

Four types of information were obtained and utilized in the model

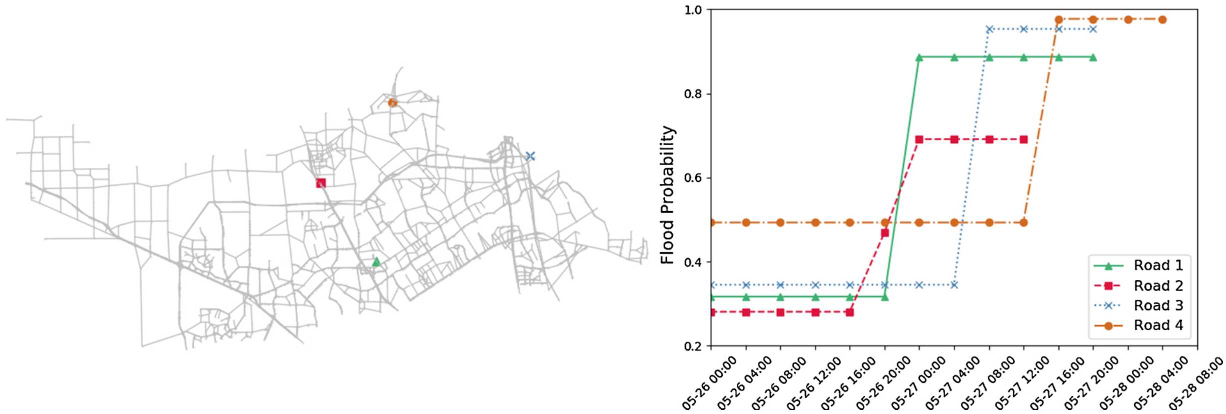

Fig. 11. Temporal failure cascade probability prediction at different road intersections.

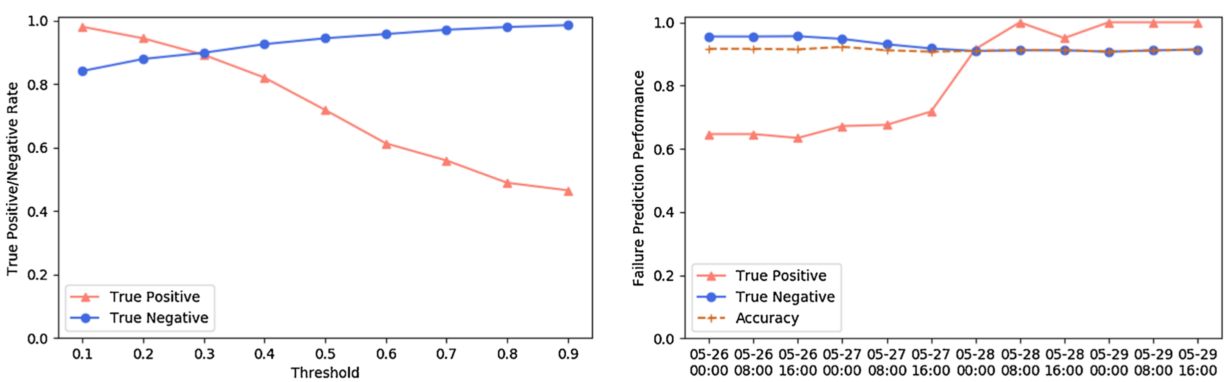

(a) Failure prediction performance at different probability thresholds

(b) Failure detection accuracy at different timestamps

Fig. 12. Failure cascade prediction performance of Bayesian network model.

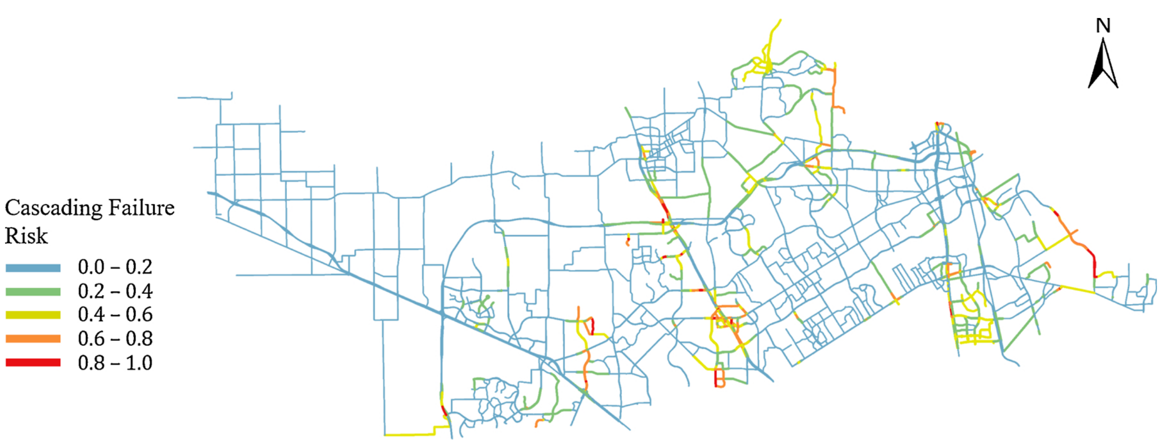

Fig. 13. Characterization of road network risk of cascading failure in flooding.

Table 1
Roads' cascading failure risk statistics.

	Cascading failure risk									
Category	0.0–0.1	0.1–0.2	0.2–0.3	0.3–0.4	0.4–0.5	0.5–0.6	0.6–0.7	0.7–0.8	0.8–0.9	0.9–1.0
Number	4703	682	288	323	359	236	215	135	70	24
Percentage	74%	10.7%	4.5%	5.1%	5.7%	3.7%	3.4%	2.1%	1.1%	0.4%

training, rainfall, channel water level, and channel and road inundation status. The first three data are collected at 30 min interval directly from Harris County Flood Warning System (HCFWS) (HCFWS, 2019). The rainfall is represented as categorical data, classified based on whether the rainfall amount in the next 12 h would exceed 6.35 cm, which is considered as moderate rainfall (NMLA, 2019). In addition, the channel water level is also transformed into a categorical format based on whether the residual height between channel water level and the top of a channel exceeds 13 cm within 6 h before overflow. Road inundation data requires additional processing. First, to determine the flood status of each road link, we extracted a series of inundation maps from HCFWS through scripting and slicing the flooding warning system. The maps are in binary format (inundated or not) with a size of 1792 × 1536 pixels. Second, the inundation maps are projected to the road network to identify the inundated roads. The inundation data for every 30 min were retrieved and processed. Finally, we used data from the Tax Day flood and Hurricane Harvey flood as the training set and Memorial Day flood as the test set. The training step estimates the conditional probability distribution for each variable based on the given data set, and the prediction step uses the variable elimination algorithm to compute the probability given evidence. Our Bayesian network model has 127 sensors and 4061 road intersections. We used an AWS t2.2xlarge instance (8 cores and 32 GB memory with up to 3.0 GHz Intel scalable processor) and it took about 3 min for the training process and 5 s for the prediction of each intersection.

4.1. Road network failure cascade probability prediction

Using the 2016 Tax Day flood and 2016 Hurricane Harvey flood trained Bayesian network model, we predicted the 2016 Memorial Day flood cascade and compared with the empirical flood propagation. Fig. 10(a) shows the predicted flooding probability at each intersection, with the darker shades of blue indicating the value of the probability (only nodes with probability large than 0.5 are plotted). Fig. 10(b) shows the empirical flood in a four-hour interval, with green nodes indicating the non-flooded road intersections. In both figures, red nodes represent the flooded road intersections. Comparing the failure cascade forecast and empirical flood inundation (focusing on the blue markers highlighted with orange box), we can see that predicted high failure probability nodes are flooded in the following time stamps. The results show the capability of the proposed Bayesian network model in predicting the failure cascade dynamics in a co-located flood control-road network.

Zooming into different road intersections, Fig. 11 shows the time series of the predicted failure probability during the course of the flood event. The endpoint of the probability curve marks the inundation of the road intersection. The probability information enables us to determine the likelihood of flooding in a road intersection. This information is critical for emergency response teams during the unfolding of a flood event.

4.2. Failure cascade characterization performance

To devise the predicted failure set, we adopted a threshold-based technique (Eq. (4)) to determine the failure nodes set. p_c is the probability threshold. When the predicted flooding probability p exceeds the threshold, the road intersection is predicted to be flooded in the future.

$$p_f = \begin{cases} 0 \text{ (Not failed)} & p < p_c \\ 1 \text{ (Failed)} & p \geq p_c \end{cases} \tag{4}$$

The selection of threshold p_c influences the model prediction performance, such as the true positive rate (TPR) and true negative rate (TNR). Fig. 12 shows the failure (i.e., flooding) prediction performance at different values of p_c. There exists a trade-off point in which the model achieves both good TPR and TNR (shown in Fig. 12(a)). In this case, 0.3 is selected as the threshold for the combined watershed. The threshold can, however, be adjusted based on a decision-maker's tolerance for uncertainty. A higher threshold can be chosen to ensure a greater correct prediction rate. Fig. 12(b) presents the failure prediction performance at different time steps with a flooding probability threshold of 0.3. The accuracy of the prediction is measured by Eq. (5). Fig. 12(b) shows that the proposed model can achieve very good results in terms of characterizing and predicting the road failure cascade process.

$$\text{Accuracy} = \frac{\sum \text{True positive} + \sum \text{True negative}}{\sum \text{Total population}} \tag{5}$$

4.3. Road network cascading failure risk assessment

Based on the trained co-located channel-road Bayesian network model, we can derive the risk of road network to cascading failure (Algorithm (2)). Essentially, a road's cascading failure risk is measured based on the marginal flooding probability difference of its nearby channel being flooded and not flooded. This flooding probability difference captured the influence of co-location dependency between channel and road networks. Fig. 13 shows the cascading failure risk map of the road network with the colors representing the magnitude of inundation risks.

According to the distribution of road cascading failure risk presented in Table 1, 16.4% of the links exhibit very high risk values (greater than 0.4), which suggests that they are highly exposed to cascading failure due to the overflow in flood control network. The road network cascading failure risk map in Fig. 13 illustrates these roads with high cascading failure risk which are located near the critical intersections of the network. The derived road cascading failure risk map could provide the decision-makers with a risk-informed tool to prioritize the emergency response in disaster management and infrastructure protection in the hazard mitigation plan.

5. Concluding remarks

This proposed road network cascading failure risk assessment in urban flooding compliments the existing approaches by considering the failure influence from its co-located flood control infrastructures. The proposed Bayesian network model of co-located channel-road network enables the integration of both static features such as topology of both networks and the dynamic features such as empirical flooding propagation to derive the cascading failure risk of road network. Departing from the standard risk exposure assessment in Fig. 1 where road only has a binary status of in flood-prone area or not, our proposed cascading failure risk assessment in Fig. 13 provides a tiered representation of risks in road networks. A link's flood risk is obtained based on its location in the network, the influence of its co-located channel network, as well as historical flooding evidence. The improved quantitative measure of the flood risk allows decision-makers to prioritize the infrastructure protections, which can help optimize the allocation of the limited resources for flood risk reduction and hazard mitigation planning. In addition, the high accuracy prediction (around 90%) for road failures obtained by the proposed Bayesian network model can provide early warning information regarding the potential flooding of roads to help communities and emergency responders to better respond to floods and the resulting road inundations.

Although this paper used Harris County as the test-bed, the proposed framework can be adapted to other regions. To further improve the model performance, the results can benefit from adding extra sensors to the flood control network. So far, there are 28 sensors in the studied watershed installed to date. However, back to the time when Memorial Day and Tax Day floods occurred, some of the sensors had not been installed. Therefore, we do not have the flooding history related to those newly installed sensors, which is the reason why we only used data from 20 sensors instead of all the 28 sensors. We have experimented with 12 sensors and 5 flood events, but the model performance deteriorated and was incapable of detecting the initial flood occurring with low true positive rates, which shows the importance of having more sensors to have better model performance. In fact, after the disastrous impact of Hurricane Harvey, Harris County Flood Control District installed several more sensors to have a better monitoring of the flood risk. However, due to the installation and maintenance cost, they did not install as many sensors as need. The number of sensors (i.e., 20) does not provide the required observability for monitoring the status of the channel network, however, for this study, we could only use these data to learn from the past events and predict the future flood risks. Despite the limited number of sensors, we were able to achieve decent results from the proposed Bayesian model. In order to better inform future sensor installation, an ongoing work by the authors is analyzing the network observability of installed 20 sensors using network control theory to derive a more effective sensor network configuration. (e.g., number of sensors, location). The current study provides a base model for flood prediction in co-located road and channel networks and could be improved and updated once more sensors are installed and more data of the flood events are collected.

Additionally, due to the data limitation (e.g., channel slope, elevation, material friction, etc.) to calculate the intermediate node water depth, an interpolation method is employed in this paper using a linear relationship assumption which cannot fully capture the flow dynamics of the channel. Despite the simplification on the water depth approximation, the proposed Bayesian network modeling framework effectively captures the co-location interdependency between channel network and road network and shows good performance in characterizing the flood cascading on the road network and predicting future flooding. Through the use the proposed framework, future studies could further improve the performance of the model with more data from flood events and more accurate water depth calculation in the future. More features, such as land use, can also be incorporated to accurately characterize the flow dynamics of the study area in the future. Besides, several parameters were categorized during the Bayesian modeling approach. This approach sacrificed data resolution that can potentially impact the prediction results. Therefore, future studies could examine other modeling techniques such as deep learning and spatial-temporal neural network to improve cascading failure prediction. Moreover, the proposed cascading failure analysis can be integrated with other measures in the future, such as criticality in providing access to critical facilities (hospitals) and the social vulnerability of the region to further specify flood risk cascade in urban areas.

Declaration of Competing Interest

The authors report no declarations of competing interest.

Acknowledgement

The authors would like to acknowledge funding support from the National Science Foundation RAPID project #1760258: “RAPID: Assessment of Risks and Vulnerability in Coupled Human-Physical Networks of Houston's Flood Protection, Emergency Response, and Transportation Infrastructure in Harvey”, and CRISP 2.0 Type 2 #1832662: “Anatomy of Coupled Human-Infrastructure Systems Resilience to Urban Flooding: Integrated Assessment of Social, Institutional, and Physical Networks”. Any opinions, findings, and conclusion or recommendations expressed in this research are those of the authors and do not necessarily reflect the view of the funding agencies.

References

Abebe, Y., Kabir, G., & Tesfamariam, S. (2018). Assessing urban areas vulnerability to pluvial flooding using gis applications and Bayesian belief network model. *Journal of Cleaner Production, 174*, 1629–1641.

Aerts, J. C., Botzen, W. J., Clarke, K. C., Cutter, S. L., Hall, J. W., Merz, B., et al. (2018). Integrating human behaviour dynamics into flood disaster risk assessment. *Nature Climate Change, 8*, 193–199.

Al-Sabhan, W., Mulligan, M., & Blackburn, G. A. (2003). A real-time hydrological model for flood prediction using gis and the www. *Computers, Environment and Urban Systems, 27*, 9–32.

Applegate, C. J., & Tien, I. (2018). Framework for probabilistic vulnerability analysis of interdependent infrastructure systems. *Journal of Computing in Civil Engineering, 33*, 04018058.

Batouli, M., & Mostafavi, A. (2018). Multiagent simulation for complex adaptive modeling of road infrastructure resilience to sea-level rise. *Computer-Aided Civil and Infrastructure Engineering, 33*, 393–410.

Bensi, M. T., Der Kiureghian, A., & Straub, D. (2011). *A Bayesian network methodology for infrastructure seismic risk assessment and decision support.* Pacific Earthquake Engineering Research Center PEER Report.

Berdica, K. (2002). An introduction to road vulnerability: What has been done, is done and should be done. *Transport Policy, 9*, 117–127.

Berke, P. R., Malecha, M. L., Yu, S., Lee, J., & Masterson, J. H. (2019). Plan integration for resilience scorecard: Evaluating networks of plans in six us coastal cities. *Journal of Environmental Planning and Management, 62*, 901–920.

Birkmann, J. (2007). Risk and vulnerability indicators at different scales: Applicability, usefulness and policy implications. *Environmental Hazards, 7*, 20–31.

Chang, L., Peng, F., Ouyang, Y., Elnashai, A. S., & Spencer, B. F., Jr. (2012). Bridge seismic retrofit program planning to maximize postearthquake transportation network capacity. *Journal of Infrastructure Systems, 18*, 75–88.

Chang, T. J., Wang, C. H., & Chen, A. S. (2015). A novel approach to model dynamic flow interactions between storm sewer system and overland surface for different land covers in urban areas. *Journal of Hydrology, 524*, 662–679.

Chen, J., Zhong, P. A., An, R., Zhu, F., & Xu, B. (2019). Risk analysis for real-time flood control operation of a multi-reservoir system using a dynamic Bayesian network. *Environmental Modelling & Software, 111*, 409–420.

Dey, A. K., Gel, Y. R., & Poor, H. V. (2019). What network motifs tell us about resilience and reliability of complex networks. *Proceedings of the National Academy of Sciences United States of America, 116*, 19368–19373.

Di Giorgio, A., & Liberati, F. (2012). A Bayesian network-based approach to the critical infrastructure interdependencies analysis. *IEEE Systems Journal, 6*, 510–519.

Dong, S., Esmalian, A., Farahmand, H., & Mostafavi, A. (2020). An integrated physical-social analysis of disrupted access to critical facilities and community service-loss tolerance in urban flooding. *Computers, Environment and Urban Systems, 80*, 101443.

Dong, S., Mostafizi, A., Wang, H., Gao, J., & Li, X. (2020). Measuring the topological robustness of transportation networks to disaster-induced failures: A percolation approach. *Journal of Infrastructure System*.

Dong, S., Wang, H., Mostafavi, A., & Gao, J. (2019). Robust component: A robustness measure that incorporates access to critical facilities under disruptions. *Journal of the Royal Society Interface, 16*, 20190149.

Dong, S., Wang, H., Mostafizi, A., & Song, X. (2020). A network-of-networks percolation analysis of cascading failures in spatially co-located road-sewer infrastructure networks. *Physica A: Statistical Mechanics and Its Applications, 538*, 122971.

Dong, S., Yu, T., Farahmand, H., & Mostafavi, A. (2019). Bayesian modeling of flood control networks for failure cascade characterization and vulnerability assessment. *Computer-Aided Civil and Infrastructure Engineering,* 1–17.

Erath, A., Birdsall, J., Axhausen, K. W., & Hajdin, R. (2009). Vulnerability assessment methodology for swiss road network. *Transportation Research Record, 2137*, 118–126.

Gehl, P., Cavalieri, F., Franchin, P., & Negulescu, C. (2017). Robustness of a hybrid simulation-based Bayesian approach for the risk assessment of a real-world road network. In: *Proc. of the 12th international conf. on structural safety and reliability*.

Gehl, P., & D'Ayala, D. (2016). Development of Bayesian networks for the multi-hazard fragility assessment of bridge systems. *Structural Safety, 60*, 37–46.

Goldbeck, N., Angeloudis, P., & Ochieng, W. Y. (2019). Resilience assessment for interdependent urban infrastructure systems using dynamic network flow models. *Reliability Engineering & System Safety, 188*, 62–79.

González, A. D., Sánchez-Silva, M., Due nas-Osorio, L., & Medaglia, A. L. (2014). *Mitigation strategies for lifeline systems based on the interdependent network design problem. Vulnerability, uncertainty, and risk: Quantification, mitigation, and management*762–771.

Gori, A., Blessing, R., Juan, A., Brody, S., & Bedient, P. (2019). Characterizing urbanization impacts on floodplain through integrated land use, hydrologic, and hydraulic modeling. *Journal of Hydrology, 568*, 82–95.

Grande, Z., Castillo, E., Mora, E., & Lo, H. K. (2017). Highway and road probabilistic safety assessment based on Bayesian network models. *Computer-Aided Civil and Infrastructure Engineering, 32*, 379–396.

Haraguchi, M., & Kim, S. (2016). Critical infrastructure interdependence in new york city during hurricane sandy. *International Journal of Disaster Resilience in the Built Environment, 7*, 133–143.

HCFCD (2019). *Harris county flood control district, hurricane harvey* see http://www.hcfcd.org/Portals/62/Harvey/immediate-flood-report-final-hurricane-harvey-2017.pdf.

HCFWS (2019). *Harris county flood control district, Harris County flood warning system.* see https://www.harriscountyfws.org.

Hossain, N. U. I., Jaradat, R., Hosseini, S., Marufuzzaman, M., & Buchanan, R. K. (2019). A framework for modeling and assessing system resilience using a Bayesian network: A case study of an interdependent electrical infrastructure system. *International Journal of Critical Infrastructure Protection, 25*, 62–83.

Hosseini, S., & Barker, K. (2016). Modeling infrastructure resilience using Bayesian networks: A case study of inland waterway ports. *Computers & Industrial Engineering, 93*, 252–266.

Itoh, T., Ikeda, A., Nagayama, T., & Mizuyama, T. (2018). Hydraulic model tests for propagation of flow and sediment in floods due to breaking of a natural landslide dam during a mountainous torrent. *International Journal of Sediment Research, 33*, 107–116.

Jenelius, E., & Mattsson, L. G. (2015). Road network vulnerability analysis: Conceptualization, implementation and application. *Computers, Environment and Urban Systems, 49*, 136–147.

Jenelius, E., Petersen, T., & Mattsson, L. G. (2006). Importance and exposure in road network vulnerability analysis. *Transportation Research Part A: Policy and Practice, 40*, 537–560.

Johansson, J., & Hassel, H. (2010). An approach for modelling interdependent infrastructures in the context of vulnerability analysis. *Reliability Engineering & System Safety, 95*, 1335–1344.

Joo, H., Choi, C., Kim, J., Kim, D., Kim, S., & Kim, H. S. (2019). A Bayesian network-based integrated for flood risk assessment (infra). *Sustainability, 11*, 3733.

Joyce, J., Chang, N. B., Harji, R., & Ruppert, T. (2018). Coupling infrastructure resilience and flood risk assessment via copulas analyses for a coastal green-grey-blue drainage system under extreme weather events. *Environmental Modelling & Software, 100*, 82–103.

Khakzad, N. (2015). Application of dynamic Bayesian network to risk analysis of domino effects in chemical infrastructures. *Reliability Engineering & System Safety, 138*, 263–272.

Klinkhamer, C., Krueger, E., Zhan, X., Blumensaat, F., Ukkusuri, S., & Rao, P. S. C. (2017). *Functionally fractal urban networks: Geospatial co-location and homogeneity of infrastructure.* (arXiv preprint) arXiv:1712.03883.

Konduri, K. C., Pendyala, R. M., You, D., Chiu, Y. C., Hickman, M. D., Noh, H., et al. (2013). Network-sensitive transport modeling framework for evaluating impacts of network disruptions on traveler choices under varying levels of user information provision. *Transportation research board 92nd annual meeting*.

Li, L., Wang, J., Leung, H., & Jiang, C. (2010). Assessment of catastrophic risk using Bayesian network constructed from domain knowledge and spatial data. *Risk Analysis: An International Journal, 30*, 1157–1175.

Little, J. C., Hester, E. T., Elsawah, S., Filz, G. M., Sandu, A., Carey, C. C., et al. (2019). A tiered, system-of-systems modeling framework for resolving complex socio-environmental policy issues. *Environmental Modelling & Software, 112*, 82–94.

Lü, H., Hou, T., Horton, R., Zhu, Y., Chen, X., Jia, Y., et al. (2013). The streamflow estimation using the xinanjiang rainfall runoff model and dual state-parameter estimation method. *Journal of Hydrology, 480*, 102–114.

Lyu, H. M., Shen, S. L., Zhou, A. N., & Zhou, W. H. (2019). *Flood risk assessment of metro systems in a subsiding environment using the interval fahp-fca approach.* Sustainable Cities and Society101682.

Mostafavi, A. (2017). A system-of-systems approach for integrated resilience assessment in highway transportation infrastructure investment. *Infrastructures, 2*, 22.

Mostafavi, A. (2018). A system-of-systems framework for exploratory analysis of climate change impacts on civil infrastructure resilience. *Sustainable and Resilient Infrastructure, 3*, 175–192.

Mostafavi, A., & Ganapati, N. E. (2019). Toward convergence disaster research: Building integrative theories using simulation. *Risk Analysis,* 1–9.

Mostafizi, A., Wang, H., Cox, D., Cramer, L. A., & Dong, S. (2017). Agent-based tsunami evacuation modeling of unplanned network disruptions for evidence-driven resource allocation and retrofitting strategies. *Natural Hazards, 88*, 1347–1372.

Narayan, S., Simmonds, D., Nicholls, R. J., & Clarke, D. (2018). A Bayesian network model for assessments of coastal inundation pathways and probabilities. *Journal of Flood Risk Management, 11*, S233–S250.

NMLA (2019). *National meteorological library and archives, fact sheet no. 3 – Water in the atmosphere.* see http://www.metoffice.gov.uk/media/pdf/4/1/No._03_-_Water_in_the_Atmosphere.pdf.

Oh, E. H., Deshmukh, A., & Hastak, M. (2010). Vulnerability assessment of critical infrastructure, associated industries, and communities during extreme events. *Construction research congress 2010: Innovation for reshaping construction practice,* 449–469.

Rahimi, M., Dehghani, N. L., & Shafieezadeh, A. (2019). Probabilistic lifecycle cost analysis of levees against backward erosion. *International conference on sustainable infrastructure 2019* (pp. 566–574).

Rahnamay-Naeini, M., & Hayat, M. M. (2016). Cascading failures in interdependent infrastructures: An interdependent markov-chain approach. *IEEE Transactions on Smart Grid, 7*, 1997–2006.

Rasoulkhani, K., & Mostafavi, A. (2018). Resilience as an emergent property of human-infrastructure dynamics: A multi-agent simulation model for characterizing regime shifts and tipping point behaviors in infrastructure systems. *PLOS ONE, 13*, e0207674.

Saidi, S., Kattan, L., Jayasinghe, P., Hettiaratchi, P., & Taron, J. (2018). Integrated infrastructure systems-a review. *Sustainable Cities and Society, 36*, 1–11.

Saliminejad, S., & Gharaibeh, N. G. (2012). A spatial-Bayesian technique for imputing pavement network repair data. *Computer-Aided Civil and Infrastructure Engineering, 27*, 594–607.

Scutari, M., & Nagarajan, R. (2013). Identifying significant edges in graphical models of molecular networks. *Artificial Intelligence in Medicine, 57*, 207–217.

Seyoum, S. D., Vojinovic, Z., Price, R. K., & Weesakul, S. (2012). Coupled 1d and non-inertia 2d flood inundation model for simulation of urban flooding. *Journal of Hydraulic Engineering, 138*, 23–34.

Singh, P., Sinha, V. S. P., Vijhani, A., & Pahuja, N. (2018). Vulnerability assessment of urban road network from urban flood. *International Journal of Disaster Risk Reduction, 28*, 237–250.

Špačková, O., & Straub, D. (2013). Dynamic Bayesian network for probabilistic modeling of tunnel excavation processes. *Computer-Aided Civil and Infrastructure Engineering, 28*, 1–21.

Sullivan, J. L., Novak, D. C., Aultman-Hall, L., & Scott, D. M. (2010). Identifying critical road segments and measuring system-wide robustness in transportation networks with isolating links: A link-based capacity-reduction approach. *Transportation Research Part A: Policy and Practice, 44*, 323–336.

Tasdighi, A., Arabi, M., Harmel, D., & Line, D. (2018). A bayesian total uncertainty analysis framework for assessment of management practices using watershed models. *Environmental Modelling & Software, 108*, 240–252.

Taylor, M. A. (2012). Network vulnerability in large-scale transport networks. *Transportation Research Part A, 5*, 743–745.

Taylor, M. A., Sekhar, S. V., & D'Este, G. M. (2006). Application of accessibility based methods for vulnerability analysis of strategic road networks. *Networks and Spatial Economics, 6*, 267–291.

Thacker, S., Barr, S., Pant, R., Hall, J. W., & Alderson, D. (2017). Geographic hotspots of critical national infrastructure. *Risk Analysis, 37*, 2490–2505.

Wang, W., Yang, S., Stanley, H. E., & Gao, J. (2019). Local floods induce large-scale abrupt failures of road networks. *Nature Communications, 10*, 2114.

Winn, J., & Bishop, C. M. (2005). Variational message passing. *Journal of Machine Learning Research, 6*, 661–694.

Yang, Y., Ng, S. T., Zhou, S., Xu, F. J., & Li, H. (2019a]). A physics-based framework for analyzing the resilience of interdependent civil infrastructure systems: A climatic extreme event case in Hong Kong. *Sustainable Cities and Society, 47*, 101485.

Yang, Y., Ng, S. T., Zhou, S., Xu, F. J., & Li, H. (2019b]). *Physics-based resilience assessment of interdependent civil infrastructure systems with condition-varying components: A case with stormwater drainage system and road transport system.* Sustainable Cities and Society101886.

Yin, J., Yu, D., Yin, Z., Liu, M., & He, Q. (2016). Evaluating the impact and risk of pluvial flash flood on intra-urban road network: A case study in the city center of shanghai, china. *Journal of Hydrology, 537*, 138–145.

Zhu, J., Manandhar, B., Truong, J., Ganapati, N. E., Pradhananga, N., Davidson, R. A., et al. (2017). Assessment of infrastructure resilience in the 2015 Gorkha, Nepal, earthquake. *Earthquake Spectra, 33*, S147–S165.